http://dx.doi.org/10.5012/bkcs.2013.34.3.753

Diffusion of CO_2 Molecules in Polyethylene Terephthalate/Polylactide Blends Estimated by Molecular Dynamics Simulations

Li-Qiong Liao,[†,‡] Yi-Zheng Fu,[†,‡] Xiao-Yan Liang,[†,‡] Lin-Yu Mei,[†,‡] and Ya-Qing Liu[†,‡,*]

[†]*School of Materials Science and Engineering, North University of China, Taiyuan, Shanxi 030051, P.R. China*
[*]*E-mail: zfflyq98@163.com*
[‡]*Research Center for Engineering Technology of Polymeric Composites of Shanxi Province, North University of China, Taiyuan, Shanxi 030051, P.R. China*
Received September 21, 2012, Accepted December 5, 2012

Molecular dynamics (MD) simulations have been used to study the diffusion behavior of small gas molecules (CO_2) in polyethylene terephthalate (PET)/polylactide (PLA) blends. The Flory-Huggins interaction parameters (χ) determined from the cohesive energy densities are smaller than the critical value of Flory-Huggins interaction parameters ($\chi_{critical}$), and that indicates the good compatibility of PET/PLA blends. The diffusion coefficients of CO_2 are determined via MD simulations at 298 K. That the order of diffusion coefficients is correlated with the availably fractional free volume (FFV) of CO_2 in the PET/PLA blends means that the FFV plays a vital role in the diffusion behavior of CO_2 molecules in PET/PLA blends. The slopes of the log (MSD) as a function of log (t) are close to unity over the entire composition range of PET/PLA blends, which confirmes the feasibility of MD approach reaches the normal diffusion regime of CO_2 in PET/PLA blends.

Key Words : Molecular modeling, Compatibility, Polymer blend, Diffusion

Introduction

In recent years, the quality of polymer-made bottles containing liquids has been improved, and the demand for them is also increasing. For various reasons, drinks have often been stored in plastic bottles, so there is a need to limit the CO_2 loss due to the relatively high permeability of such material. Blending different polymers has been widely used to obtain products with desirable properties that are not necessarily possessed by an individual component polymer. The case-study involves the blends of polyethylene terephthalate (PET), which is commonly used for food packaging and drinks storage[1-3] and polylactide (PLA), a biodegradable green polyester derived from renewable resources, but relatively more expensive.[4,5] Cebe[3] has studied the non-isothermal crystallization of PET/PLA blends by differential scanning calorimetry (DSC) and X-ray scattering over a wide composition range from 0% to 100% PLA. For food packaging, in particular for drinks storage, the most important characteristic of a blend is its barrier property. The accurate knowledge of such microcosmic properties is extremely important for technological applications, since these properties determine their processability as well as final product properties.

With the ever-growing computational power and the development of theoretical models, molecular dynamics (MD) simulations have become powerful tools and are playing an increasingly important role in materials modeling and related technology development, as they provide structural and dynamic details of certain material at a molecular scale that have been inaccessible or difficult to be obtained with experimental techniques. Generally, the important factor that determines the properties of a blend is the compatibility of polymer pairs. Up to now, most of the studies have reported that MD simulations have recently been successfully used to investigate the compatibility of polymer blends[6-8] and to obtain the diffusion coefficients of small molecules in pure polymers,[9-15] polymer blends,[16,17] organic-inorganic hybrid members.[18] For example, Luo[8] investigated the miscibility of PEO/PVC blends by MD simulations. It was found that PEO/PVC 70/30 and 30/70 blends are more miscible than 50/50 blend by the Flory-Huggins parameters determined from the cohesive energy densities and the radial distribution functions of the inter-molecular atoms. Chen[9] adopted MD simulations to study the permeability of CO_2/CH_4 in three PAIs isomers, 6FDA/8p, 6FDA/8m and 6FDA/12p, and the results were close to the reported experimental data. And Pan[17] investigated the diffusion behavior of water vapor/propylene in PVA-P (AA-AMPS) blend membranes by MD simulations. The results showed the same changing trends with that of the experimental results. To the best of our knowledge, the compatibility of PET/PLA blends and diffusion behavior of gas molecules in PET/PLA blends have never been investigated at a molecular scale. In order to understand and predict the diffusion coefficients of CO_2 in PET/PLA blends, it is very desirable to use molecular simulation method to explore the effects of polymer blend ratio on the compatibility of PET/PLA blends and the diffusion behavior of CO_2 in them from a molecular point of view through MD simulations. The results can be used to improve the knowledge on gas diffusion behavior through polymer blends.

Model and Simulation Details

Amorphous Cells Building. The chemical structures of PET, PLA used in this study are shown in Figure 1. PET/PLA blends are constructed by the following weight ratios of PET to PLA: 100/0, 90/10, 70/30, 50/50, 30/70, 10/90, and 0/100. In MD simulations, short chains may lead to end effects and cannot represent the real systems accurately. On the other hand, one also wants to avoid using very long chains because of computer datastorage space limitations and simulation time. In our previous investigation,[19] we have found that 20 repeat units could represent PET and PLA chains. Moreover, Pavel[20] chose polymer chain with polymerization degree ranging from 20 to 60 as a PET chain to study the diffusion of small molecule penetrants in models of PET. Sarasua[7] found that 20 repeat units were sufficient for PLA to perform the simulations for the analysis and prediction of miscibility in PLA/PVPh blends. Thus, 20 repeat units are chosen as PET and PLA chains in this study. The number of units, chains and initial densities are summarized in Table 1. The densities of PET,[21] PLA[4] are set as 1.330 g·cm^{-3} and 1.248 g·cm^{-3}, respectively. Densities of the blends are calculated from the densities of individual polymer and volume fractions of each polymer.

All simulations are carried out using the Materials Studio (MS) software package from Accerlys Inc. The Amorphous Cell module of MS is used to construct the 20 initial structures of polymers. Periodic boundary conditions are applied to the cubic simulations cells at 298 K. To eliminate the unfavorable contacts, and the 20 configurations are subjected to the energy minimization (with the steepest descent, conjugate gradient, and Newton methods in cascade). Next, the lowest energy configuration is chosen for a 1000 ps-NPT (T = 500 K, P = 1 bar) MD simulation and then a 10-cycle thermal annealing is conducted from 300 K to 1000 K and then back to 300 K with 50 K intervals. The duration of the NPT (P = 1 bar) MD simulation at each temperature is 10 ps. Afterward, 500 ps NPT (T = 298 K, P = 1 bar) and 500 ps NVT (T = 298 K) MD simulations are carried out. Trajectories are saved every 1 ps and the final 300 ps configurations are used to analyze characteristic of the blends.

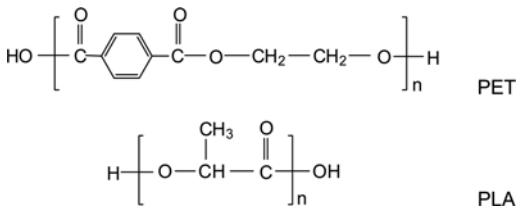

Figure 1. Chemical structures of PET and PLA.

COMPASS[22] force field is applied to calculate the interatomic interactions in this study. During the whole simulations process, the Ewald summation is adopted for the Coulombic interactions with an accuracy of 0.0001 kcal·mol^{-1}, and the Atom-based summation is applied for the van der Waals interactions with a cutoff distance of 9.5 Å, a spline width of 1 Å, and a buffer width of 0.5 Å. Pressure and temperature are controlled by the Berendsen method with decay constant 0.1 ps. The equations of motion are integrated with a time step of 1 fs for all simulations.

Simulation of Diffusivity. Diffusion coefficients are determined by adding 10 CO_2 molecules to each independently equilibrated configuration to form a new simulation cell at 298 K. After equilibrated by using the same procedure as mentioned in Section Amorphous Cells Building, each configuration is then subjected to NVT (T = 298 K) MD simulation for a total of 3500 ps.

Results and Discussion

Interaction Energy between PET and PLA. When PET is blended with PLA, inter-molecular interaction becomes very important in determining the compatibility of the blend. The interaction energy (ΔE) between PET and PLA can be calculated as follows:[23]

$$\Delta E = E_{\text{Blend}} - (E_{\text{PET}} + E_{\text{PLA}}) \quad (1)$$

where E_{Blend} is the potential energy of PET/PLA blends; E_{PET} and E_{PLA} are the potential energy of optimized PET and PLA polymer, respectively. COMPASS force field is a powerful force field supporting atomistic simulations of polymeric materials. In this study, the COMPASS force field has been used throughout the simulations except the calculation of non-bond interaction energy since the H-bond force isn't a separate term in COMPASS force field and is contained in other non-bond interaction.[24] It means COMPASS force field cannot provide the exact values of the H-bond energy of the simulated systems. To solve this problem, the Dreiding force field is introduced as a complement. The non-bond interaction energies are composed of van der Waals (E_{vdW}),

Table 1. PET/PLA blends of different compositions involved in MD simulations

System	PET/PLA compositions	Number of PLA units	Number of PET units	Number of chains	Initial density (g·cm^{-3})	Number of atoms
1	100/0	-	20	3PET	1.330	1329
2	90/10	20	34	2PET/1PLA	1.321	1685
3	70/30	20	26	2PET/3PLA	1.304	1699
4	50/50	20	23	1PET/3PLA	1.288	1058
5	30/70	20	23	1PET/7PLA	1.272	1790
6	10/90	20	20	1PET/24PLA	1.256	4835
7	0/100	20	-	8PLA	1.248	1464

Table 2. Interaction energies ΔE (kcal·mol^{-1}) between PET and PLA in PET/PLA blends

	90/10	70/30	50/50	30/70	10/90
ΔE_{Total}	-138.08 ± 5.10	-328.64 ± 24.36	-192.17 ± 9.49	-297.61 ± 22.68	-326.12 ± 25.06
$\Delta E_{H\text{-}bond}$	-1.61 ± 0.46	-13.10 ± 3.91	-5.32 ± 1.82	-9.16 ± 2.38	-6.18 ± 2.83
ΔE_{vdW}	-111.14 ± 4.72	-233.10 ± 24.62	-141.38 ± 12.21	-219.14 ± 22.93	-246.64 ± 27.76
ΔE_{Elect}	-25.33 ± 1.22	-82.43 ± 6.22	-45.46 ± 4.73	-69.31 ± 4.17	-73.31 ± 6.21

electrostatic (E_{Elect}) and H-bond ($E_{H\text{-}bond}$) interactions.

$$E_{non\text{-}bond} = E_{vdW} + E_{Elect} + E_{H\text{-}bond} \quad (2)$$

The results of the interaction energies between PET and PLA are listed in Table 2. As shown in Table 2, high amount of polar groups in PET and PLA chains form H-bonds between PET and PLA chains. When PET is blended with PLA, the H-bonds increase the interaction between PET and PLA, which contributes to the compatibility of PET/PLA blends. Both the interaction energies, van der Waals, electrostatic and H-bonds interaction energies are negative values, revealing the attractive force between PET and PLA polymer.

Compatibility of PET/PLA Blends. Flory-Huggins interaction parameter (χ) can be employed to investigate the miscibility/compatibility of a binary blend. If the binary blend is sufficiently equilibrated, the energy of mixing (ΔE_{mix}) can be calculated according to:[25]

$$\Delta E_{mix} = \phi_A\left(\frac{E_{coh}}{V}\right)_A + \phi_B\left(\frac{E_{coh}}{V}\right)_B - \left(\frac{E_{coh}}{V}\right)_{mix} \quad (3)$$

where the terms in parenthesis represent the cohesive energies density of the pure polymers (A and B) and the blend (mix); the symbols ϕ_A and ϕ_B represent the volume fractions of A and B, respectively, $\phi_A + \phi_B = 1$.

The χ can be calculated from ΔE_{mix} according to:[25]

$$\chi_{AB} = \left(\frac{\Delta E_{mix}}{RT}\right)V_{mono} \quad (4)$$

where V_{mono} is a monomer unit volume per mole; R is the molar gas constant and T is the temperature in Kelvin.

Based on the Flory-Huggins theory, in order to understand the compatibility/incompatibility behavior of PET and PLA, the critical value of Flory-Huggins interaction parameter $(\chi_{AB})_{critical}$ is calculated using the equation:

$$(\chi_{AB})_{critical} = \frac{1}{2}\left(\frac{1}{\sqrt{n_A}} + \frac{1}{\sqrt{n_B}}\right)^2 \quad (5)$$

where n_A and n_B represent the number of repeat units (actual number of repeating units) of polymer A and B, respectively. If $\chi_{AB} < (\chi_{AB})_{critical}$, the blend is considered to be compatible. If χ_{AB} is considerably greater than $(\chi_{AB})_{critical}$, then blend is incompatible. For a value of χ_{AB} slightly greater than $(\chi_{AB})_{critical}$, the blend is partially compatible. Thus, comparing the measured χ_{AB} with $(\chi_{AB})_{critical}$ provides a good indication about the compatibility of blend.[26] The results of χ_{AB} *vs* weight fraction of PLA calculated from Eq. (4) and (5) are displayed in Figure 2. In this study, all simulated χ_{AB} of the PET/PLA blends are smaller than $(\chi_{AB})_{critical}$, indicating the good compatibility of PET and PLA in the blends. It agrees well with experimental data available in literature.[3]

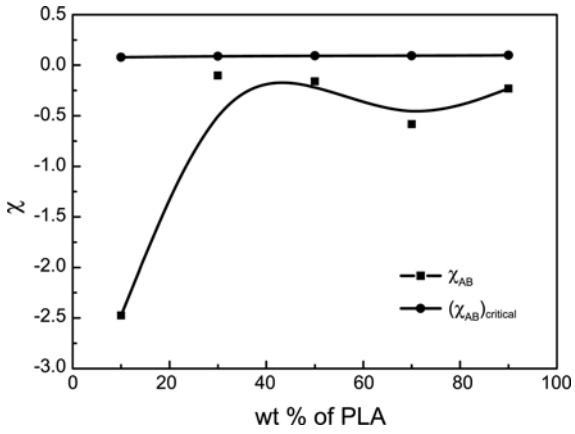

Figure 2. Flory-Huggins interaction parameter *vs* weight fraction of PLA.

Fractional Free Volume in PET/PLA Blends. Fractional free volume (FFV) plays a vital role in the diffusion behavior of gas molecules in blends, and it can be analyzed by Connolly surface method, which is the locus of the probe centre as the probe freely rolls over the framework. The gas molecules, CO_2 are selected as probe molecules which are modeled by spheres with the diameter 0.33 nm (kinetic diameter).[9] The simulated morphologies of free volumes in the well-equilibrated models of PET/PLA blends and pure PET, PLA are shown in Figure 3, the blue regions (outside of the isosurface) represent the free volume and the grey regions (inside of the isosurface) represent the occupied volume.

The results of simulated FFV that are accessible to CO_2 in PET/PLA blends are shown in Figure 4 and it follows the order of 0/100 > 90/10 > 30/70 > 10/90 > 50/50 > 70/30 > 100/0, which is the crosscurrent as Flory-Huggins interaction parameters. For models with same volume, the lower packing efficiency the smaller of FFV. But in our study, the volume of each model is various, it depends on the blend ratio and interaction between PET and PLA in PET/PLA blends. The weaker interaction (as in the case of 90/10 PET/PLA blend) reduces the packing efficiency, which results in a looser structure and a larger FFV. When PET-PLA interaction becomes stronger (as in the case of 70/30 PET/PLA blend), the molecules are packed more tightly with each other, thus free volume voids become much less than that in the case of 90/10 PET/PLA blend, namely, the FFV is smaller than that in 90/10 PET/PLA blend. Thereby, the change of FFV depends heavily on the interaction of PET/PLA blends.

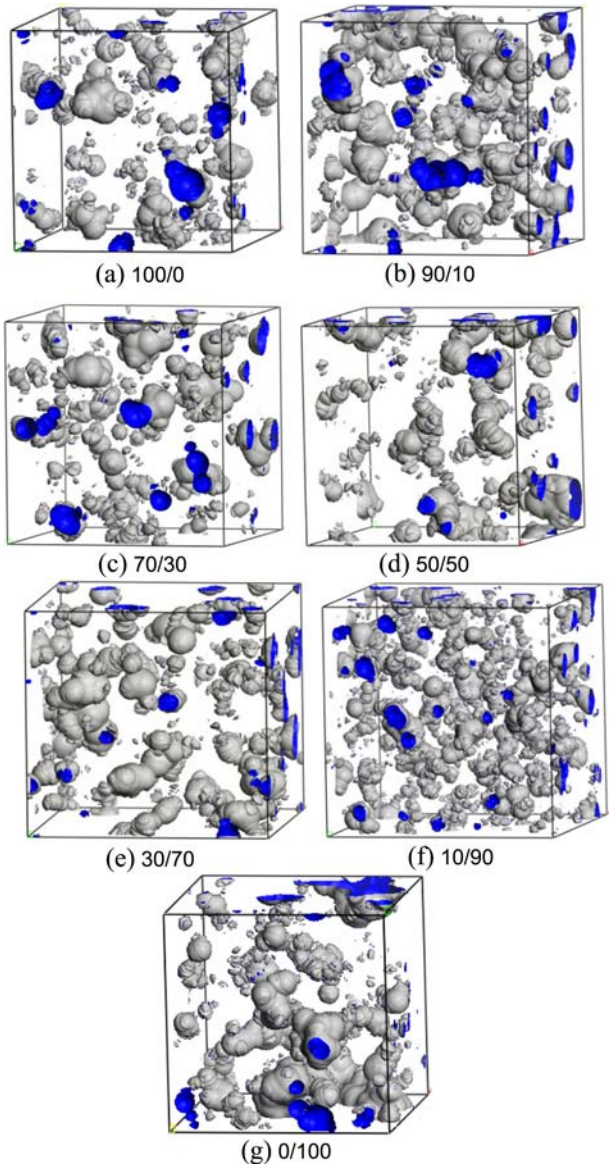

Figure 3. Simulated morphologies of free volumes in the well-equilibrated models of PET/PLA blends.

Diffusion Coefficient from Simulation. Diffusion coefficient is easily obtained through calculating the mean-square displacement of the respective penetrant during the MD runs, and it can be calculated by the Einstein relation:[27]

$$D = \frac{1}{6N}\lim_{t\to\infty}\frac{d}{dt}\sum_{i=1}^{N}\langle|R(t)-R(0)|^2\rangle \quad (6)$$

where D represents the diffusion coefficient of penetrant; $|R(t)-R(0)|^2$ is the mean-square displacement (MSD); $R(t)$ and $R(0)$ are positions of the center of mass of a penetrant at time t and 0, respectively; $\langle\cdots\rangle$ is the last-squares fit of the mean-square displacements of centers of mass of the penetrant averaged over all possible time origins, namely, means the ensemble average.

The diffusion coefficients of CO_2 in the blends of PET/PLA are listed in Table 3. Free volume properties are the main factors that determine the diffusion of CO_2 in PET/PLA blends. The simulated diffusion coefficients of CO_2 in PET/PLA blends increase by the order of 90/10 > 30/70 > 10/90 > 50/50 > 70/30, showing the identical tendency as the FFV, that is, the larger the FFV in blends, the greater diffusion coefficient of CO_2. It indicates that the FFV plays the most important role in the process of diffusion. Higher FFV means more accessible free volume voids in the blends for CO_2 diffusion. Meanwhile, higher FFV indicates that the free volume voids connect with each other easily to form large voids, which might enhance the diffusivity of CO_2. Consequently, the diffusion coefficients of CO_2 in the blends of PET/PLA depend heavily on the FFV of PET/PLA blends. As shown in Table 3, 70/30 PET/PLA blend has a lower CO_2 diffusion coefficient and offeres very high barrier properties of CO_2. The simulated diffusion coefficients of CO_2 in the pure polymers, PET and PLA are larger compared with the experimental data since there are still some significant differences in the scale between the simulated model and the actual system, such as the finite polymer chains used in the MD simulation, the lower density of the simulated system as compared to the experimental density and the fact that the amorphous configurations generated by the Amorphous Cell program are "too amorphous" while the experimental diffusion coefficients are measured in the presence of crystalline phase, thus it has some difficulties in obtaining really polymeric materials.[14,15,28] Besides, some of

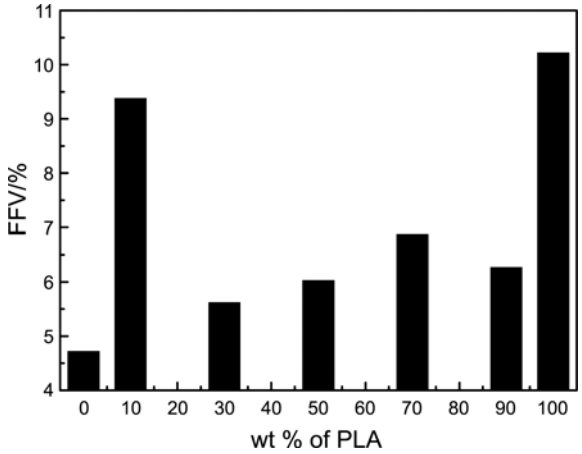

Figure 4. The simulated FFV of the PET/PLA blends measured by a probe of size of CO_2.

Table 3. Diffusion coefficients for CO_2 in PET/PLA blends

System	D (10^{-11} m^2·s^{-1})	exp (10^{-13} m^2·s^{-1})
100/0	2.43	1.00[30]
90/10	10.75	-
70/30	2.67	-
50/50	2.95	-
30/70	6.80	-
10/90	6.35	-
0/100	11.42	4.80 ± 0.47[31]

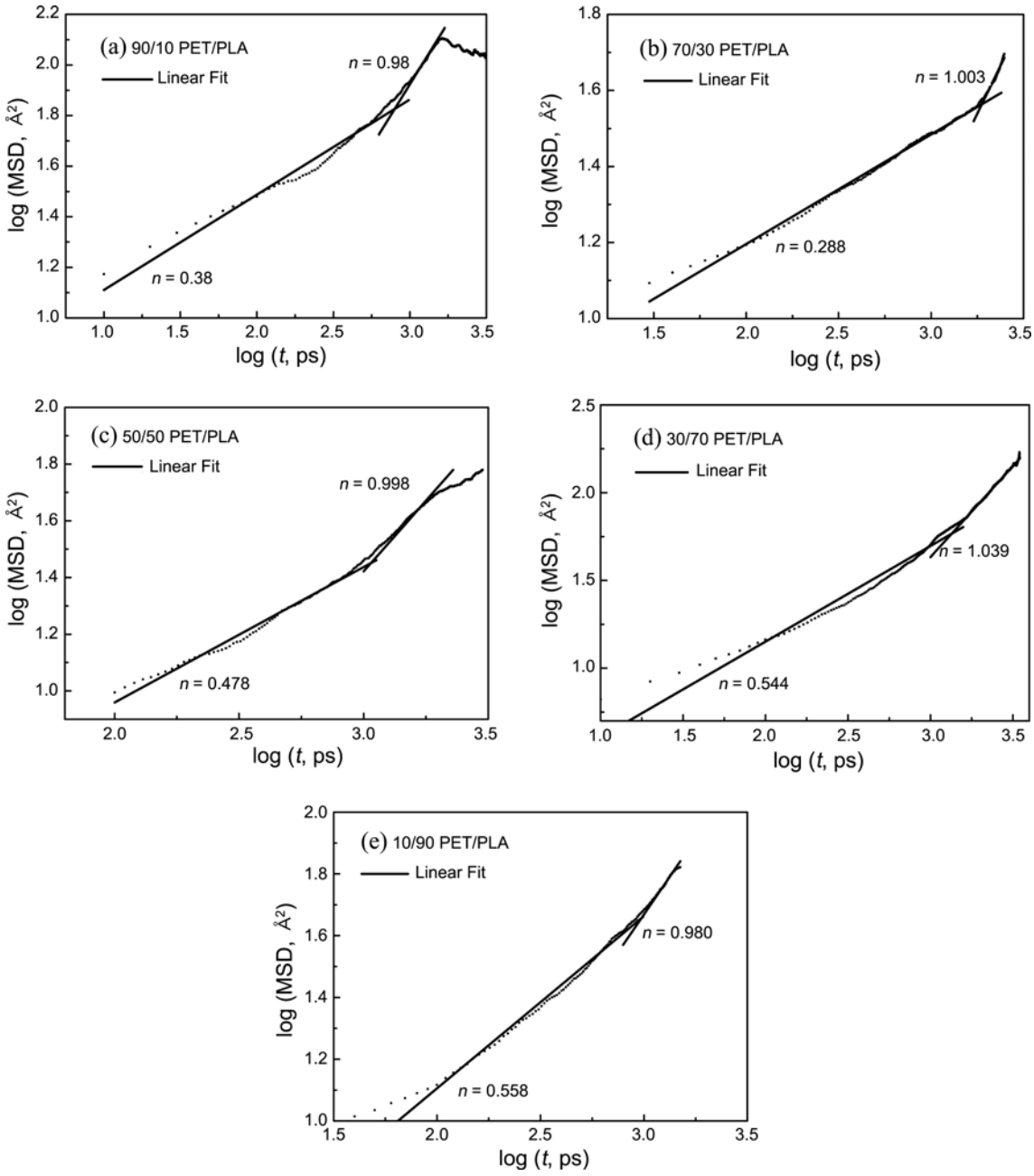

Figure 5. Log(MSD) *vs* log(*t*) plots for the diffusion of CO_2 in PET/PLA blends.

the approximations and assumptions in the computational model possibly result in the discrepancy. A similar discrepancy has already been reported in the literature.[9,14,15,29] However, the trend of the simulated diffusion coefficients of pure PET and PLA agrees well with the experimental data, namely, the diffusion coefficient of CO_2 in PET is smaller than that in PLA.

The time dependence of the log(MSD) of CO_2 molecules in PET/PLA are presented in Figure 5. The criterion for a model system reaching the normal diffusion regime is the slope of log(MSD) *vs* log(*t*) approaches unity.[32] From Figure 5, the slope of the log(MSD) *vs* log(*t*) curve increases approximately to unity after long time MD simulation over the entire composition range of PET/PLA blends. This result confirms the feasibility of MD approach to reach the normal diffusion regime of CO_2 in PET/PLA blends.

Conclusion

In this study, MD simulations are performed to study the compatibility of PET/PLA blends and the diffusion behavior of CO_2 in the PET/PLA blends at the molecular scale. The calculation results of interaction energy show that there are attractive force between PET and PLA polymer. That all simulated χ_{AB} of the PET/PLA blends are smaller than $(\chi_{AB})_{critical}$ ensures the desirable compatibility in the blends, which is in fair agreement with the experimental data in literature. Simulated fractional free volume (FFV) that are

accessible to CO_2 in PET/PLA blends follows the order of 0/100 > 90/10 > 30/70 > 10/90 > 50/50 > 70/30 > 100/0. And the ratio dependence of diffusion coefficients is related to the FFV of PET/PLA blends. Higher FFV means more accessible free volume voids and the free volume voids can easily connect with each other to form large voids in the PET/PLA blends for CO_2 diffusion, that is, the higher FFV of PET/PLA, the larger diffusion coefficient of CO_2 in the blends, indicating the lower barrier property of CO_2.

References

1. Wang, Q. F.; Keffer, D. J.; Nicholson, D. M.; Thomas, J. B. *Macromolecules* **2010**, *43*, 10722.
2. Welle, F. *Resour. Conserv. Recy.* **2011**, *51*, 865.
3. Chen, H. P.; Pyda, M.; Cebe, P. *Thermochim. Acta* **2009**, *492*, 61.
4. Auras, R.; Harte, B.; Selke, S. *Macromol. Biosci.* **2004**, *4*, 835.
5. Nampoothiri, K. M.; Nair, N. R.; John, R. P. *Bioresour. Technol*. **2010**, *101*, 8493.
6. Jing, J.; Qiao, Q. A.; Jin, Y. Q.; Ma, C. H.; Cai, H. L.; Meng, Y. F.; Cai, Z. T.; Feng, D. C. *Chin. J. Chem*. **2012**, *30*, 133.
7. Arenaza, I. M.; Meaurio, E.; Coto, B.; Sarasua, J. R. *Polymer* **2010**, *51*, 4431.
8. Luo, Z. L.; Jiang, J. W. *Polymer* **2010**, *51*, 291.
9. Chen, Y.; Liu, Q. L.; Zhu, A. M.; Zhang, Q. G.; Wu, J. Y. *J. Membr. Sci*. **2010**, *348*, 204.
10. Mozaffari, F.; Eslami, H.; Moghadasi, J. *Polymer* **2010**, *51*, 300.
11. Jawalkar, S. S.; Aminabhavi, T. M. *Polym. Int.* **2007**, *56*, 928.
12. Harmandaris, V. A.; Adhikari, N. P.; van der Vegt, N. F. A.; Kremer, K. *Macromolecules* **2007**, *40*, 7026.
13. Harmandaris, V. A.; Angelopoulou, D.; Mavrantzas, V. G.; Theodorou, D. N. *J. Chem. Phys.* **2002**, *116*, 7656.
14. Müller-Plathe, F. *J. Chem. Phys.* **1991**, *94*, 3192.
15. Takeuchi, H.; Roe, R. J.; Mark, J. E. *J. Chem. Phys.* **1990**, *93*, 9042.
16. Pavel, D.; Shanks, R. *Polymer* **2005**, *46*, 6135.
17. Pan, F. S.; Ma, J.; Cui, L.; Jiang, Z. Y. *Chem. Eng. Sci.* **2009**, *64*, 5192.
18. Pan, F. S.; Peng, F. B.; Lu, L. Y.; Wang, J. T.; Jiang, Z. Y. *Chem. Eng. Sci*. **2008**, *63*, 1072.
19. Liao, L. Q.; Fu, Y. Z.; Liang, X. Y.; Liu, Y. Q. *Polym. Mat. Sci. Eng*. **2012**, *28*, 170.
20. Pavel, D.; Shanks, R. *Polymer* **2003**, *44*, 6713.
21. McGonigle, E. A.; Liggat, J. J.; Pethrick, R. A.; Jenkins, S. D.; Daly, J. H.; Hayward, D. *Polymer* **2001**, *42*, 2413.
22. Sun, H. *J. Phys. Chem. B* **1998**, *102*, 7338.
23. Mohanty, S.; Nando, G. B. *Polymer* **1996**, *37*, 5387.
24. Fang, Z. P. *Molecular Dynamics Simulation on Silicon Rubber Pervaporation Membranes and their Diffusion Properties*; Tianjin University, Tianjin, 2008.
25. Case, F. H.; Honeycutt, J. D. *Trends Polym. Sci*. **1994**, *2*, 259.
26. Jawalkar, S. S.; Aminabhavi, T. M. *Polymer* **2006**, *47*, 8061.
27. Lu, C. H.; Ni, S. J.; Chen, W. K.; Liao, J. S.; Zhang, C. J. *Comput. Mater. Sci*. **2010**, *49*, S65.
28. Tocci, E.; Bellacchio, E.; Russo, N.; Drioli, E. *J. Membr. Sci*. **2002**, *206*, 389.
29. Pant, P. V. K.; Boyd, R. E. *Macromolecules* **1992**, *25*, 494.
30. Okuji, S.; Sekiya, M.; Nakabayashi, M.; Endo, H.; Sakudo, N.; Nagai, K. *Instrum. Methods Phys. Res., Sect. B* **2006**, *242*, 353.
31. Komatsuka, T.; Kusakabe, A.; Nagai, K. *Desalination* **2008**, *234*, 212.
32. Liu, Q. L.; Huang, Y. *J. Phys. Chem. B* **2006**, *110*, 17375.